HHS Public Access

Author manuscript

Cytometry A. Author manuscript; available in PMC 2016 May 09.

Published in final edited form as:

Cytometry A. 2015 May ; 87(5): 419–427. doi:10.1002/cyto.a.22658.

Visualization of Pulmonary Clearance Mechanisms via Noninvasive Optical Imaging Validated by Near-Infrared Flow Cytometry

Haiying Zhou[1], **Sean P. Gunsten**[2], **Natalia G. Zhegalova**[1], **Sharon Bloch**[1], **Samuel Achilefu**[1], **J. Christopher Holley**[3], **Daniel Schweppe**[3], **Walter Akers**[1], **Steven L. Brody**[1,2], **William Eades**[2,3,*], and **Mikhail Y. Berezin**[1,*]

[1]Department of Radiology, Washington University School of Medicine, St. Louis, MO

[2]Department of Medicine, Washington University School of Medicine, St. Louis, MO

[3]Siteman Cancer Center Flow Cytometry Core, Washington University School of Medicine, St. Louis, MO

Abstract

In vivo optical imaging with near-infrared (NIR) probes is an established method of diagnostics in preclinical and clinical studies. However, the specificities of these probes are difficult to validate ex vivo due to the lack of NIR flow cytometry. To address this limitation, we modified a flow cytometer to include an additional NIR channel using a 752 nm laser line. The flow cytometry system was tested using NIR microspheres and cell lines labeled with a combination of visible range and NIR fluorescent dyes. The approach was verified in vivo in mice evaluated for immune response in lungs after intratracheal delivery of the NIR contrast agent. Flow cytometry of cells obtained from the lung bronchoalveolar lavage demonstrated that the NIR dye was taken up by pulmonary macrophages as early as four-hours post-injection. This combination of optical imaging with NIR flow cytometry extends the capability of imaging and enables complementation of in vivo imaging with cell-specific studies.

Keywords

Near-infrared; in vivo imaging; flow cytometry; alveolar macrophage; lung imaging

Introduction

Clinical and preclinical diagnostics based on optical molecular imaging requires use of contrast agents in the near-infrared (NIR) spectral range (700-900 nm) (1,2). Due to low absorbance, attenuated scattering, and minimal autofluorescence, relatively large depth

*Corresponding authors: William Eades (eadesb@wustl.edu), **Contact information:** Mikhail Berezin, PhD, Assistant Professor, Department of Radiology, Washington University School of Medicine, 510 S. Kingshighway, Barnard Bldg, 6th floor, 6604A, St. Louis, MO 63110, USA, phone: 314.747.0701, fax: 314.747.5190, (berezinm@mir.wustl.edu).

Conflict of Interest

The authors declare no conflict of interest

penetration of NIR photons (up to several centimeters) can be achieved (3,4). In particular, planar reflectance imaging in living animals enables high throughput and longitudinal detection of fluorescent reporter distribution in organs and tissues (5). However, due to the highly heterogeneous nature of biological tissues, cell-specific accumulation of the contrast agent can be difficult to assess in living organisms.. Specificity is currently semi-quantitatively measured via fluorescence intensity in the 2-dimensional region of interest in live animals, requiring excision of organ tissues for gross biodistribution analysis (6). Following excision, NIR fluorescence microscopy of thin tissue sections and isolated cells is conducted to determine the localization of the signal in the targeted tissue and verify the uptake of the probe by cells of interest. These microscopy techniques do not provide detailed cellular information, since the population of cells studied by microscopy is generally low and obscured by the resolution provided by the methodology. More reliable and cell-specific information could be provided by flow cytometry operated in the same NIR spectral channel as optical imaging. This information would allow multi-parametric, simultaneous analysis of thousands of cells to determine cell morphology, cell distribution, antigen expression, and many other physical, chemical, and biological characteristics.

Realizing the importance of NIR flow cytometry, a few descriptions of NIR measurements with NIR-labeled cells have been published (7-9). The methods either utilized tandem probes (9,10) allowing excitation with a standard red laser using unmodified flow cytometers or explored alternative detectors such as CCD cameras with holographic grating (7) and avalanche photodiodes (8). None of these approaches allow the use of commercial flow cytometers for NIR probe excitation. To address this problem, we have modified the light source of a commonly used flow cytometry system to include a 752 nm laser line from a krypton laser and corresponding NIR compatible optics. NIR fluorescence detection of this modified flow cytometry system was then tested with NIR fluorescent polystyrene microspheres and was further validated on several cell lines labeled with both visible and NIR fluorophores. Following instrument validation, a strategy that included in vivo optical imaging and flow cytometry was performed to investigate the uptake and track the fate of the contrast agent in lungs during clearance. The approach is outlined in **Figure 1**. The NIR contrast agent selected from the cell studies showed strong uptake by macrophages was administered intratracheally to the lungs of mice. The contrast agent's biodistribution was monitored in vivo by NIR imaging longitudinally. During this process, the cells from lungs were sampled using bronchoalveolar lavage and stained with the macrophage specific antibodies labeled with a fluorophore emitting in the red channel. Finally, flow cytometry in NIR and red channels was performed to demonstrate the uptake of the contrast probe by immune cells.

EXPERIMENTAL DATA

Materials

Polybead® Amino 6.0 micron microspheres in water were obtained from Polyscience, Inc (cat. #19118). LS601-NHS ester was prepared as previously described (11), cypate was synthesized as reported (4). 1-Ethyl-3-[3-dimethylaminopropyl]carbodiimide hydrochloride (EDC) was obtained from Sigma-Aldrich. Lysotracker Red was purchased from Life

Technologies. Ultrapure water (18.2 MΩ·cm, Millipore) was used in this work for synthesis and buffer preparations. Solvents were obtained from ThermoFisher Scientific. Absorption spectra were recorded using UV-Vis spectrophotometer Beckman Coulter DU-640. Steady state fluorescence spectra were recorded on a Nanolog spectrofluorometer (Horiba Jobin Yvon, Inc.) equipped with an R928 photomultiplier tube (PMT) that is commonly used in the characterization of NIR contrast agents and nanoparticles (12). The same type of PMT tube was used in the modified flow cytometer (see below).

Flow cytometer

A MoFlo HTS cell sorter (Beckman Coulter) was equipped with an I-90C Krypton-ion laser (Coherent) and modified to detect NIR. This laser has the capability of mirror and coupler changes to create a 752 nm single wavelength output (optics kit part #0156-459-30, Coherent). After modifications, the Krypton-ion laser produced 212 mW of single line 752 nm light (see the spectrum in Supporting Information, **Figure S1**) with a fully open (10/10) aperture. The wavelength of the laser was measured using a UCB2000+UV-Vis spectrophotometer (Ocean Optics) with grating sensitivity to NIR (400-1000 nm)

The modified system uses a high energy NIR laser that is not visible to the human eye and may cause severe burns to skin and the eye. Protective goggles rated for NIR were used in these studies.

Formation of a TEM-00 beam profile required constraining the laser output to a smaller aperture (value of 3/10), in turn reducing laser power to 115 mW. Laser power loss through three translation mirrors was less than 4% cumulative. The greatest loss was incurred by the beam focusing lens, which accounted for slightly more than 20% loss. Laser power was serially reduced from its maximum to determine excitation saturation of the NIR dye, which was 75 mW. Alignment aids included an infrared detection card (part #VRC5, Thorlabs) and Fluoresbrite Carboxylate alignment monodisperse microspheres 1.75 μm (ex. 763 nm, em 820 nm) - (cat #17690-1, Polysciences).

Photomultiplier modules H957-15 with R928 photomultiplier tubes (Hamamatsu Photonics) were utilized for their known, although limited sensitivity in NIR bandwidth. Given relatively weak (~ 30% at 800 nm and 10% at 850 nm) and understood variable efficiency and wavelength response peaks of R928 PMTs, we used a number of H957-15 modules with R928 PMTs and rotated them into the NIR position until the best response was received. Filters and other optical elements are discussed in the Results and Discussion section.

Synthesis and characterization of NIR fluorescent beads

A solution containing commercial beads was mixed by vortexing for 20 sec to obtain a uniform suspension and 30 μL of the suspension was placed into a 100 μL Eppendorf tube. Sodium bicarbonate buffer (40 μL, 0.1M), prepared fresh and kept at 4 °C was added to the vial. A solution of LS601-NHS in DMSO (molar excess) was added to the vial, followed by addition of 4.0 eq. of EDC. The vial was wrapped in foil and placed in the multi-tube vortex mixer (VX-2500, VWR Scientific) at a moderate speed for 3 hours. The solution was centrifuged at 6000*g* for 5 min and supernatant was removed. The remaining beads were

washed with water three-to-five times, followed by centrifugation at 6000*g* for 5 min, until no fluorescence of the liquid was observed.

The dye-free suspension of beads was collected, stored in water and used within a week of preparation. The size of the beads was measured in water by dynamic light scattering on a Zetasizer Nano ZS (Malvern). Labeling of the beads with a NIR dye was confirmed by fluorescence microscopy. For that, a drop of the bead suspension was placed on a glass slide and viewed under a coverslip using an Olympus BX51 equipped with a Cy7-B-OMF filter cube (Semrock). Flow cytometry of beads was performed with the modified NIR flow cytometer described above.

Validation of flow cytometer performance with cell lines

GFP transfected U87 glioblastoma and A427-7 human lung adenocarcinoma cells were cultured in 6-well plates. Cells were treated overnight with 500 nM Lysotracker red, ex/em 647/688 nm, (Life Technology). For NIR labeling, cells were treated overnight with 1 μM cypate. Cells were released from plates using trypsin, spun down and resuspended in PBS. For microscopic analysis, an aliquot of each treatment condition was plated on a Lab-Tek slide and visualized with an Olympus BX51 epifluorescent microscope using GFP (480/40 ex, 535/50 em), Cy5 (620/60 ex, 700/75 em) and indocyanine green (775/50 ex, 845/855 em) filter cubes.

In vivo studies

In vivo cypate delivery—All animal studies were performed in compliance with guidelines set forth by the NIH Office of Laboratory Animal Welfare and approved by the Animal Studies Committee of the Washington University School of Medicine. C57BL/6J mice, 8-10 weeks of age, were obtained from Jackson Laboratory and housed in a barrier facility. Mice were anesthetized with intraperitoneal injection of a ketamine (80 mg/kg) and xylazine (16 mg/kg) prior to neck dissection and cannulation of the trachea with a 22-gauge, 1” plastic angiocatheter. Mouse hair obstructs light transmission and was therefore removed from the ventral and dorsal skin of the thorax by gentle clipping and application of cream depilatory. The trachea and lungs were then instilled with 30 μL of 60 μM cypate in 20% DMSO (v/v in water) by micropipette injection into the catheter at a rate of 10 μL / minute. Control mice were treated with 20% DMSO in water. The catheter was removed, the wound closed with tissue adhesive, and the mice allowed to recover.

Optical imaging of mice—Fluorescence imaging of mice was performed using the Pearl Imager NIR fluorescence imaging system (Li-COR), with excitation at two different wavelengths, 685 and 785 nm, and corresponding emission collected at 710 and 810 nm, respectively. Mice were anesthetized using 2% isoflurane at 1 L/min and hair removed over the thorax by gentle clipping and application of cream depilatory. The right lateral, dorsal, and ventral aspects of the mice were imaged sequentially using the Pearl NIR imaging system before IT cypate injection, immediately after, 4 h, and 24 h post-injection. After the final scan, anesthetized mice were euthanized by cervical dislocation. Quantitative image analysis of the mice was performed using Pearl Cam Software (Li-COR).

Bronchoalveolar lavage and lung cell harvest—Four or 24 hours post-delivery of cypate, the mice were euthanized and the trachea was cannulated with a 20 gauge, 1” plastic angiocatheter. The lungs were then lavaged three times with 1 mL each of cold phosphate-buffered saline (PBS). The three aliquots of bronchoalveolar lavage (BAL) were pooled and kept on ice. The BAL was centrifuged, the supernatant discarded, and the cell pellet resuspended in 1 mL of PBS for cytocentrifuge preparation for flow cytometry. Following BAL, whole lung was excised and minced with scissors before digestion via incubation in RPMI 1640 medium (Cellgro) containing collagenases and proteases (0.28 U/mL Liberase Blendzymes, (Roche) and DNase (5 U/mL, Sigma-Aldrich) for 1 hour at 37 °C. The digested lung tissue was then passed through a 70 μm cell strainer and treated with ACK lysing buffer (Lonza) to obtain a red blood cell-free, single cell suspension for cytospin preparation.

Flow cytometry of cells from lung cell harvest—Handling and immunostaining was performed as previously described to optimize maintenance of single cell suspension for flow cytometry (13,14). Cells obtained by BAL were washed twice in flow cytometry buffer (PBS with 2% fetal bovine serum) and incubated with rat anti-mouse CD16/CD32 antibodies to block Fc receptors (Mouse BD Fc Block, BD Biosciences) for 15 min at room temperature. The cells were washed and then immunostained for 30 min at room temperature with rat anti-mouse F4/80 (AbDSerotec) antibody conjugated with Allophycocyanin (APC) fluorescent dye (abs 650, em 660) to label lung macrophages. Cells were subsequently kept on ice between two washes with flow cytometry buffer, mixed by vortex to maintain single cell suspension and analyzed by flow cytometer.

RESULTS AND DISCUSSION

Flow cytometer modification

The largest challenge for detecting NIR signals with commercially available flow cytometers, even current production, involves optical elements that do not consider laser wavelengths above 647 nm, and fluorescent emissions above 800 nm. Much of the laser and emission paths require replacement of components and choosing a light path option with the least amount of “glass” between the emission source and detection, to reduce emission loss and refractive chromatic aberration.

A benefit of using a gas-ion laser such as the Coherent I-90C-Krypton is that prismatic wavelength selection when a “single line holder” is used creates a truly single wavelength output, and does not require “clean up” filtering that subsequent solid state lasers demand. Still, we observed the output directly from the laser snout and at the flow cell with a spectrophotometer to confirm no lower wavelength energy that could potentially interfere with other parameters, or possible laser wavelength changes from the mirrors and lenses, the results directly from the laser shown in **Figure S1**.

MoFlo cell sorters use a laser translation tower comprised of either two or three mirrors to direct the laser to the height of the flow cell. However, none of the translation mirrors supplied by the manufacturer reflect a 752 nm laser beam. Existing mirrors were replaced by

ultra-broadband mirrors (part #MM2-311.12.5, Semrock) with nearly flat reflection across a 350-1100 nm bandwidth, resulting in negligible laser power loss.

A beam shaping optic (BSO) is typically used for the MoFlo systems to display an evenly distributed elliptical pattern of the laser beam across the cell stream. Having a 752 nm specific lens set to create an ellipse against the stream would be ideal for the instrument performance, however, commercial BSO assemblies or components for laser wavelengths higher than 647 nm are not available. Alternatively we used a focusing lens assembly, which required attention to the laser beam's working distance and convergence to the cell stream. Monitoring light scatter pulse width and understanding physical lens stage travel, we did not allow the beam to diverge before hitting the cell stream.

Legacy MoFlo and MoFlo XDP cell sorters incorporate three laser intercept “pinholes” spaced 50 um apart. The outer pinholes and respective emission paths are diverted 90 degrees by prisms to save space on the emission breadboard. For the NIR development we chose the “center” pinhole which allows the emission to travel directly from its origin, minimizing loss or further chromatic aberration.

This center emission path was originally designed for UV excitation and came “stock” with a two PMT array schematically shown in **Figure 2**, this emission circuit matched our need for simplicity and ability to troubleshoot interference. Our final design used a T770lpxr dichroic beam-splitter centered at 770 nm, and an HQ820/60 emission filter (Chroma Technology). The reflective side of the 770 nm dichroic was used to detect any lower wavelength interference that could affect other parameters. The detectors in the NIR emission path as well as representative parameters from the two remaining laser intercepts were measured both through the prevailing pulse processing circuit within the MoFlo and directly off of the PMT using an oscilloscope.

Testing the NIR flow cytometry with NIR microbeads

Latex microbeads labeled with the NIR dye LS601 (the structure is shown in Supporting Information, **Figure S2, A**) were utilized for the initial testing of the system. The dye has an absorption maximum at 750 nm, corresponding to the laser line of the instrument and emission maximum at 800 nm (**Figure S2, B**). Activatable carboxylic groups on the beads facilitated coupling of LS601 to amines using a standard NHS - EDC technique (11,15-17). Successful conjugation was verified by fluorescence microscopy that showed fluorescence in the NIR range (**Figure S2, D-F**). The beads retained their spherical shape and uniform size distribution of ca. 5 μm as measured by microscopy and a light scattering technique (**Figure S2, C**). NIR flow cytometry of beads carrying NIR dyes demonstrated emission signal consistent with the uniform distribution of the labeled beads and fluorescence signal in the NIR channel two orders of magnitude higher than that of unstained beads with clear separation of response against a blank bead reference (**Figure 3**).

The relatively low flow cytometry signal of the prepared NIR LS601 beads was due to relatively weak fluorescence. This weak fluorescence is common in beads labeled with NIR dyes and most likely is due to the self-quenching effect induced by close proximity of the dye molecules to each other on the particle surface (15). Optimizing synthetic conditions,

careful control of the dye-to-bead ratio, as well as new dye design with less self-quenching properties are expected to provide brighter beads.

Flow cytometry performance with NIR labeled cells

The performance of the NIR flow cytometer was next validated with cultured cell lines that were modified with fluorescent reporters in three different ranges; visible green using eGFP, visible red using a red dye cell label LysoTracker Red, and NIR using cypate (the structure is shown in **Figure 4, A**). The U87/eGFP-expressing brain cancer cells were a mixed population of eGFP positive and negative cells. These cells and the A427-7 human lung adenocarcinoma cell lines were each labeled with the LysoTracker Red probe that accumulates in acidic organelles (18). We used LysoTracker Red (abs/em 577/590 nm) to assess a potential overlap between the red and NIR channels ensuring that minimum bleed-through occurs between the channels. LysoTracker Red has an emission tail that extends to 750 nm and which may potentially interfere with the NIR readout.

Microscopy images of eGFP-expressing U87 cells stained with LysoTracker Red demonstrated two overlapping colors, corresponding to eGFP and LysoTracker Red. Flow cytometry of these cells revealed the expected populations, eGFP positive and eGFP negative, and both populations were uniformly labeled with LysoTracker Red (**Figure 4, B**). No NIR fluorescence was observed by microscopy or flow cytometry, which is consistent with the absence of a NIR dye and low bleed-through of the red emission into the NIR channel.

Cells were then incubated with the NIR dye cypate, a moderately hydrophobic contrast agent with good cell permeability and low cytotoxicity that has been intensively used for preclinical imaging of tumors (4,19). Compared to LS601 which was used to label the beads, cypate absorbance and emission were at longer wavelengths in the NIR spectrum, with an excitation maximum of 780 nm and emission at 820 nm (Supporting Information, **Figure S3**). While not attached to a targeted moiety, cypate usually demonstrates non-specific accumulation in a variety of cells, including the studied cells. Labeling of cancer cells with cypate led to the appearance of a strong signal in the NIR channel similar to LS601 (**Figure 4, C**).

Triple-labeled cells were detected by fluorescence microscopy and flow cytometry (**Figure 4, B-D**). Overlay of NIR fluorescence signal with eGFP and LysoTracker Red images visualized by microscopy was largely overlapping with the red fluorescence from LysoTracker Red, consistent with the non-specific distribution of cypate in the cell population (**Figure 4, B** and **C**). Correspondingly, flow cytometry confirmed the presence of all three fluorophores. Two populations of eGFP expressing cells (as in the above-mentioned experiment), both labeled with cypate and LysoTracker Red were seen. Similar to nontransfected U87 cells, eGFP lacking A427-7 treated with LysoTracker and cypate showed no GFP-related signal, but featured strong red and NIR signals in both microscopy and flow cytometry studies (**Figure 4, D**). Hence, both NIR and red channels showed only one, double positive population of these cells in flow cytometry experiments.

Optical imaging of lungs with a NIR dye in vivo

Based on the positive in vitro labeling results, we explored the ability of NIR flow cytometry to analyze cell populations stained in vivo. We delivered NIR dye to the lungs, taking advantage of the ability to easily access the lung's airway, and prior success in lung imaging (20). Optical imaging of lungs has great translational potential (21), driven by the development of both new optical imaging instrumentation (22,23), and novel classes of targeted imaging probes (24,25) that report on the molecular status of cells and target tissues with excellent specificity.

We were interested in the fate of the NIR dye following IT delivery and its capacity to be taken up by local lung immune cells. We used cypate, as used in vitro, since this dye is often utilized in preclinical imaging. Within four hours of IT delivery of the dye, NIR fluorescence remained localized primarily in the lungs (**Figure 5, A**), though the cellular distribution of fluorescence could not be ascertained in living animals. Longitudinal imaging of mice revealed substantially decreased levels of the NIR signal within the thorax over time (<25% of the initial total emission signal remaining at 22 h) (**Figure 5, C**). Over time, fluorescent signal could also be detected in the liver, the normal clearance pathway of cypate that not retained in the lungs (**Figure 5, A**).

Flow cytometry of the cell population obtained by bronchoalveolar lavage

Based on previous experience we anticipated that cypate molecules would be taken up by lung parenchymal cells and residential airspace macrophages within 24 hours. To determine the temporal pattern of lung immune cell uptake, cells were recovered from the lung by bronchoalveolar lavage of mice and analyzed by flow cytometry and fluorescence microscopy at 4 and 24 h post-administration. Alveolar macrophages, the major immune cells present in the alveolar air spaces, were identified using an F4/80 antibody labeled with APC fluorescent dye. The F4/80 antigen is expressed by a majority of mature alveolar macrophages and is considered a specific cell-surface marker for murine macrophages in the lung (26,27). Mice treated with cypate-free diluent showed negligible fluorescence in the NIR channel, while F4/80-positive cells could be detected in the APC channel (**Figure 6, A-B**). At 4 h after IT dye delivery, a strong fluorescent signal in the cypate channel was detected by flow cytometry in cells recovered by BAL (**Figure 6, C**). Double positive staining was observed in cells obtained from cypate-treated mice and stained with F4/80-APC. This double staining confirmed the nature of the cells with NIR fluorescence as macrophages.

At 24 h after delivery of cypate, only low levels of fluorescence were detected in the lungs by in vivo imaging. The low signal was confirmed by flow cytometry showing negligible signal from cells collected via BAL. These findings were consistent with the rapid clearance of the cells and dye from lung tissue detected by in vivo imaging in this study. By 48 h post cypate delivery, recovered cells displayed very low levels of fluorescence as detected by both in vivo imaging and NIR fluorescence microscopy and therefore, were not analyzed to flow cytometry. Thus, the 4 hour time point was found to be optimal for cypate dye uptake in alveolar macrophages, as detected by flow cytometry.

Taken together, these data show the feasibility of linking in vivo NIR imaging with cell-specific assays using readily modified standard flow cytometry instrumentation. Here, we were able to easily correlate clearance of NIR dye as detected by whole animal optical imaging with in vivo lung cell populations. We demonstrate that a lung-specific signal detected by cypate delivery can be tracked to resident alveolar macrophages using ex vivo flow cytometry. One interpretation of our findings is that the in vivo NIR signal in the lung is the sum of dye in at least two compartments: one in resident alveolar macrophages, and a second as free or a protein bound dye that rapidly transits to the circulation and the liver. We have not tracked the fate of the alveolar macrophage and cannot fully account for the loss of signal at 24 h post-delivery. It is possible that the cypate dye-laden macrophages moved out of the lungs or that the dye has moved out of the macrophage into the circulation. Recent studies of resident macrophages in the lung indicate that after latex bead or endotoxin stimulation, the alveolar macrophages remain in the lung (28,29). Thus it is more likely that the cypate fluorescence in alveolar macrophages is quenched or destroyed (for example with reactive oxygen species) or that the dye moves out of the cells, and into the circulation.

In addition to monitoring the fate of contrast agents, this approach can be extended to other areas that employ NIR imaging in the whole animal including the use of contrast agents in combination with drug delivery. This strategy affords a simple, yet efficient way of optimizing the drug delivery system by tracking the therapeutic load optically in vivo and confirming targeting ex vivo using flow cytometry (30).

Summary

We demonstrated that modification of standard flow cytometry instrumentation with a laser at 752 nm and conventional detectors allows covering a broad class of NIR probes with excitation maxima form 750 to 780 nm. Using this approach, we, for the first time, investigated the fate of an optical contrast agent delivered to the lung by the intratracheal route. Tracing these agents temporally and spatially with optical imaging techniques in vivo and ex vivo with the developed NIR flow cytometer, revealed that the delivered probes were taken up by lung macrophages. Thus, the proposed technique forms a bridge between whole-body optical imaging and cell studies to directly identify targeted cell populations and is expected to facilitate the development of contrast agents to enhance their specificities, increase target cell permeability and ultimately to reduce cell and organ toxicity.

Supplementary Material

Refer to Web version on PubMed Central for supplementary material.

Acknowledgment

We thank the Alvin J. Siteman Cancer Center at Washington University School of Medicine and Barnes-Jewish Hospital in St. Louis, Mo., for the use of the Siteman Flow Cytometry Core, The Siteman Cancer Center is supported in part by an NCI Cancer Center Support Grant #P30 CA91842. This work was also supported by the NHLBI/NIH Program of Excellence in Nanotechnology (HHSN26820). This material in part is also based upon work supported by the NSF under Award Number IIA-1355406. Any opinions, findings, and conclusions or recommendations expressed in this material are those of the author and do not necessarily reflect the views of the NSF. We also thank the Washington University Optical Spectroscopy Core Facility (NIH 1S10RR031621-01) for spectroscopy measurements.

References

1. Ahmed M, Purushotham AD, Douek M. Novel techniques for sentinel lymph node biopsy in breast cancer: a systematic review. Lancet Oncol. 2014; 15:e351–e362. [PubMed: 24988938]
2. Hilderbrand SA, Weissleder R. Near-infrared fluorescence: application to in vivo molecular imaging. Curr Opin Chem Biol. 2010; 14:71–9. [PubMed: 19879798]
3. Weissleder R, Ntziachristos V. Shedding light onto live molecular targets. Nat Med. 2003; 9:123–8. [PubMed: 12514725]
4. Achilefu S, Dorshow RB, Bugaj JE, Rajagopalan R. Novel receptor-targeted fluorescent contrast agents for in vivo tumor imaging. Invest Radiol. 2000; 35:479–85. [PubMed: 10946975]
5. Wessels JT, Busse AC, Mahrt J, Dullin C, Grabbe E, Mueller GA. In vivo imaging in experimental preclinical tumor research--a review. Cytometry A. 2007; 71A:542–9. [PubMed: 17598185]
6. Solomon M, Guo K, Sudlow GP, Berezin MY, Edwards WB, Achilefu S, Akers WJ. Detection of enzyme activity in orthotopic murine breast cancer by fluorescence lifetime imaging using a fluorescence resonance energy transfer-based molecular probe. J Biomed Opt. 2011; 16:066019. [PubMed: 21721820]
7. Nolan JP, Condello D, Duggan E, Naivar M, Novo D. Visible and near infrared fluorescence spectral flow cytometry. Cytometry A. 2013; 83A:253–64. [PubMed: 23225549]
8. Lawrence WG, Varadi G, Entine G, Podniesinski E, Wallace PK. Enhanced red and near infrared detection in flow cytometry using avalanche photodiodes. Cytometry A. 2008; 73A:767–76. [PubMed: 18612992]
9. Moore JP, Sakkal S, Bullen ML, Kemp-Harper BK, Ricardo SD, Sobey CG, Drummond GR. A flow cytometric method for the analysis of macrophages in the vascular wall. J Immunol Methods. 2013; 396:33–43. [PubMed: 23928493]
10. McLaughlin BE, Baumgarth N, Bigos M, Roederer M, De Rosa SC, Altman JD, Nixon DF, Ottinger J, Oxford C, Evans TG. Nine-color flow cytometry for accurate measurement of T cell subsets and cytokine responses. Part I: Panel design by an empiric approach. Cytometry Part A. 2008; 73A:400–410. others.
11. Gustafson TP, Cao Q, Achilefu S, Berezin MY. Defining a polymethine dye for fluorescence anisotropy applications in the near-infrared spectral range. Chemphyschem. 2012; 13:716–23. [PubMed: 22302715]
12. Nelson, W.; Winter, P.; Shokeen, M.; Wang, S.; Berezin, MY. Nanoparticles for Bioimaging: Analytical Characterization and Measurements.. In: Berezin, MY., editor. Nanotechnology for Biomedical Imaging and Diagnostics: From Nanoparticle Design to Clinical Applications. Wiley; 2014. p. 520
13. Vermaelen K, Pauwels R. Accurate and simple discrimination of mouse pulmonary dendritic cell and macrophage populations by flow cytometry: methodology and new insights. Cytometry A. 2004; 61A:170–77. [PubMed: 15382026]
14. Ibricevic A, Guntsen SP, Zhang K, Shrestha R, Liu Y, Sun JY, Welch MJ, Wooley KL, Brody SL. PEGylation of cationic, shell-crosslinked-knedel-like nanoparticles modulates inflammation and enhances cellular uptake in the lung. Nanomedicine. 2013; 9:912–22. [PubMed: 23453959]
15. Zhegalova NG, He S, Zhou H, Kim DM, Berezin MY. Minimization of self-quenching fluorescence on dyes conjugated to biomolecules with multiple labeling sites via asymmetrically charged NIR fluorophores. Contrast Media Mol Imaging. 2014; 9:355–62. [PubMed: 24764130]
16. Magalotti S, Gustafson TP, Cao Q, Abendschein DR, Pierce RA, Berezin MY, Akers WJ. Evaluation of inflammatory response to acute ischemia using near-infrared fluorescent reactive oxygen sensors. Mol Imaging Biol. 2013; 15:423–30. [PubMed: 23378226]
17. Gustafson TP, Yan Y, Newton P, Hunter DA, Achilefu S, Akers WJ, Mackinnon SE, Johnson PJ, Berezin MY. A NIR Dye for Development of Peripheral Nerve Targeted Probes. Medchemcomm. 2012; 3:685–690. [PubMed: 24575295]
18. Dolman, NJ.; Kilgore, JA.; Davidson, MW. Current Protocols in Cytometry. John Wiley & Sons, Inc.; 2001. A Review of Reagents for Fluorescence Microscopy of Cellular Compartments and Structures, Part I: BacMam Labeling and Reagents for Vesicular Structures..

19. Berezin MY, Guo K, Akers W, Livingston J, Solomon M, Lee H, Liang K, Agee A, Achilefu S. Rational approach to select small peptide molecular probes labeled with fluorescent cyanine dyes for in vivo optical imaging. Biochemistry. 2011; 50:2691–700. [PubMed: 21329363]
20. Zhou, H.; He, S.; Gunsten, S.; Brody, S.; Akers, W.; Berezin, M. OSA Technical Digest (online). Optical Society of America; San Jose, California: 2014. NIR fluorescent contrast agents for detection of inflammation of lungs in vivo.; p. AM2P.12014/06/08 OSA Technical Digest (online)
21. Dimarzio CA, Niedre M. Pre-clinical optical molecular imaging in the lung: technological challenges and future prospects. J Thorac Dis. 2012; 4:556–7. [PubMed: 23205277]
22. Takashi, A.; Takahiro, N.; Thomas, KW.; Shaf, K.; Kazuhiro, Y. Issues in Thoracic Surgery, American Thoracic Society International Conference Abstracts. American Thoracic Society; A Novel Minimally Invasive Technique For Localization Of Pulmonary Nodules Using A Near-Infrared Fluorescence Thoracoscope. D47.; p. A5830-A5830.
23. Ntziachristos V. Going deeper than microscopy: the optical imaging frontier in biology. Nat Meth. 2010; 7:603–614.
24. Bai M, Bornhop DJ. Recent advances in receptor-targeted fluorescent probes for in vivo cancer imaging. Curr Med Chem. 2012; 19:4742–58. [PubMed: 22873663]
25. Rao J, Dragulescu-Andrasi A, Yao H. Fluorescence imaging in vivo: recent advances. Curr Opin Biotechnol. 2007; 18:17–25. [PubMed: 17234399]
26. Austyn JM, Gordon S. F4/80, a monoclonal antibody directed specifically against the mouse macrophage. Eur J Immunol. 1981; 11:805–815. [PubMed: 7308288]
27. Hume DA, Robinson AP, MacPherson GG, Gordon S. The mononuclear phagocyte system of the mouse defined by immunohistochemical localization of antigen F4/80. Relationship between macrophages, Langerhans cells, reticular cells, and dendritic cells in lymphoid and hematopoietic organs. J Exp Med. 1983; 158:1522–36. [PubMed: 6355361]
28. Jakubzick C, Tacke F, Llodra J, van Rooijen N, Randolph GJ. Modulation of dendritic cell trafficking to and from the airways. J Immunol. 2006; 176:3578–84. [PubMed: 16517726]
29. Westphalen K, Gusarova GA, Islam MN, Subramanian M, Cohen TS, Prince AS, Bhattacharya J. Sessile alveolar macrophages communicate with alveolar epithelium to modulate immunity. Nature. 2014; 506:503–6. [PubMed: 24463523]
30. Vij N. Nano-based theranostics for chronic obstructive lung diseases: challenges and therapeutic potential. Expert Opin Drug Deliv. 2011; 8:1105–9. [PubMed: 21711085]

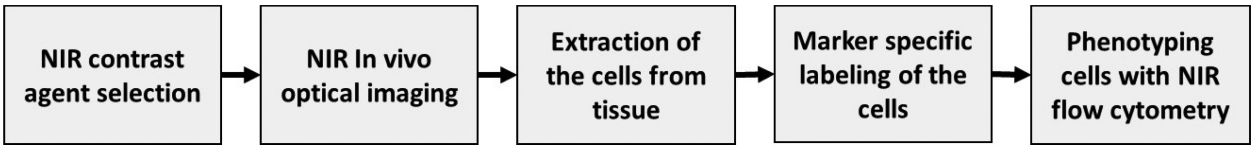

Figure 1.
Research plan to investigate the uptake of the NIR contrast agents by cells (i.e. macrophages) using NIR flow cytometry

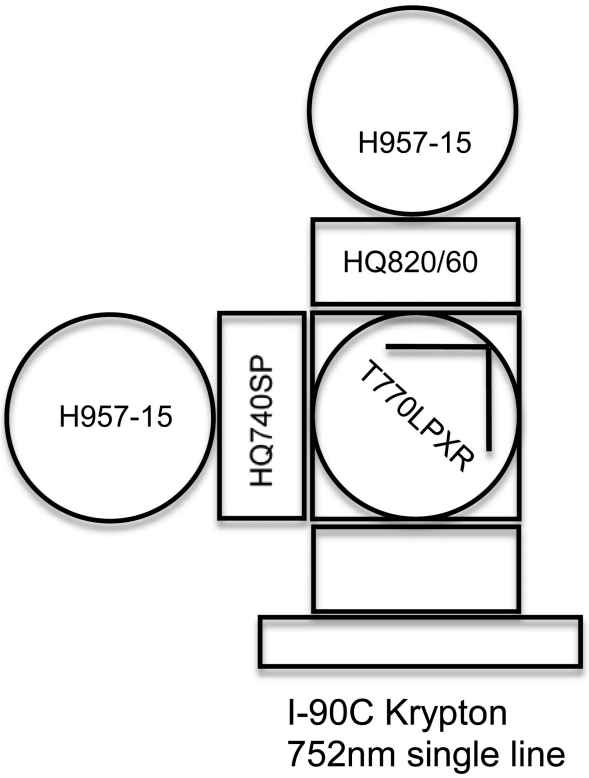

Figure 2.

Optical path diagram of the modified NIR flow cytometer that allowed observation of two emissions above 820 nm from the sample and a potential secondary emissions below 770 nm. H957-15 – a detector module with an R928 PMT, HQ820/60 - a NIR band filter. HQ740SP - a short pass filter, T770lpxr -a beam-splitter

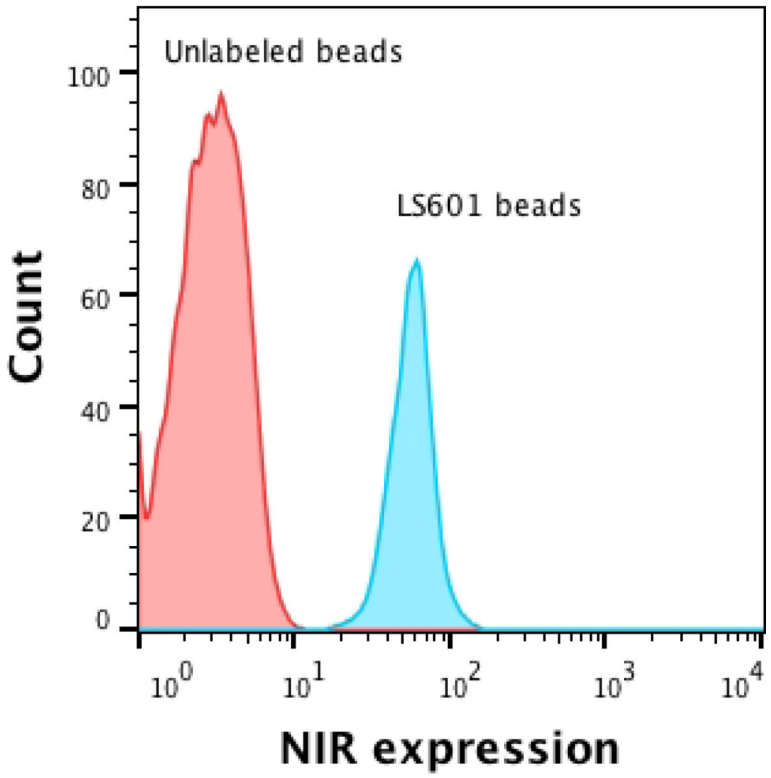

Figure 3.
NIR flow cytometry of unstained and NIR stained beads. The histograms show the number of cells vs. fluorescence signal in the NIR channel.

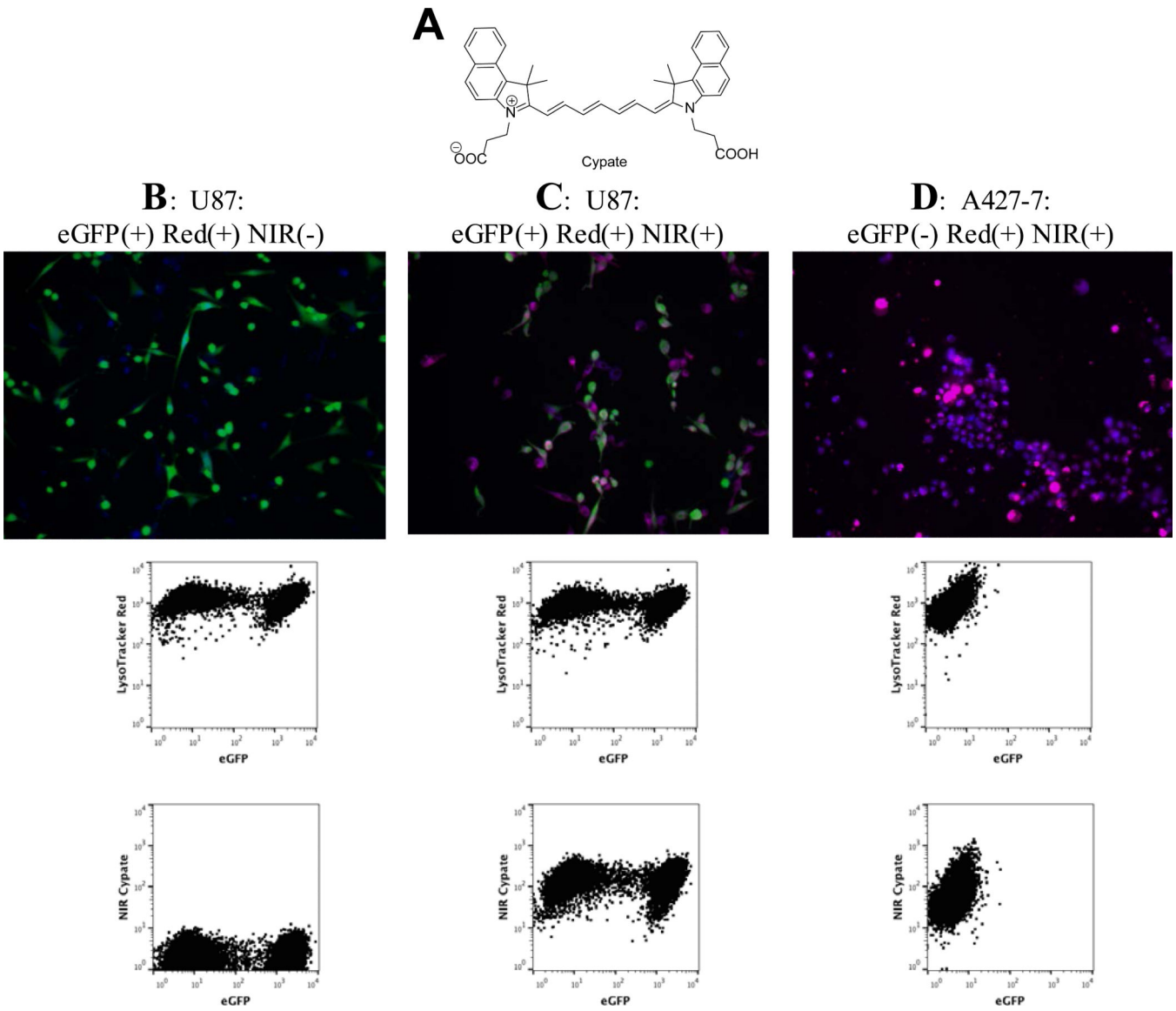

Figure 4.

Flow cytometry of fluorecently labeled cell lines. A: Structure of a NIR dye cypate, B: eGFP expressing U87 cells (green) treated with Lysotracker Red (blue); no fluorescence in NIR channel, C: U87 eGFP cells (green) + Lysotracker Red (blue) + cypate (red); D: No eGFP expressing cells A427-7 cells + Lysotracker Red (blue) + cypate (red); no fluorescence in eGFP channel.

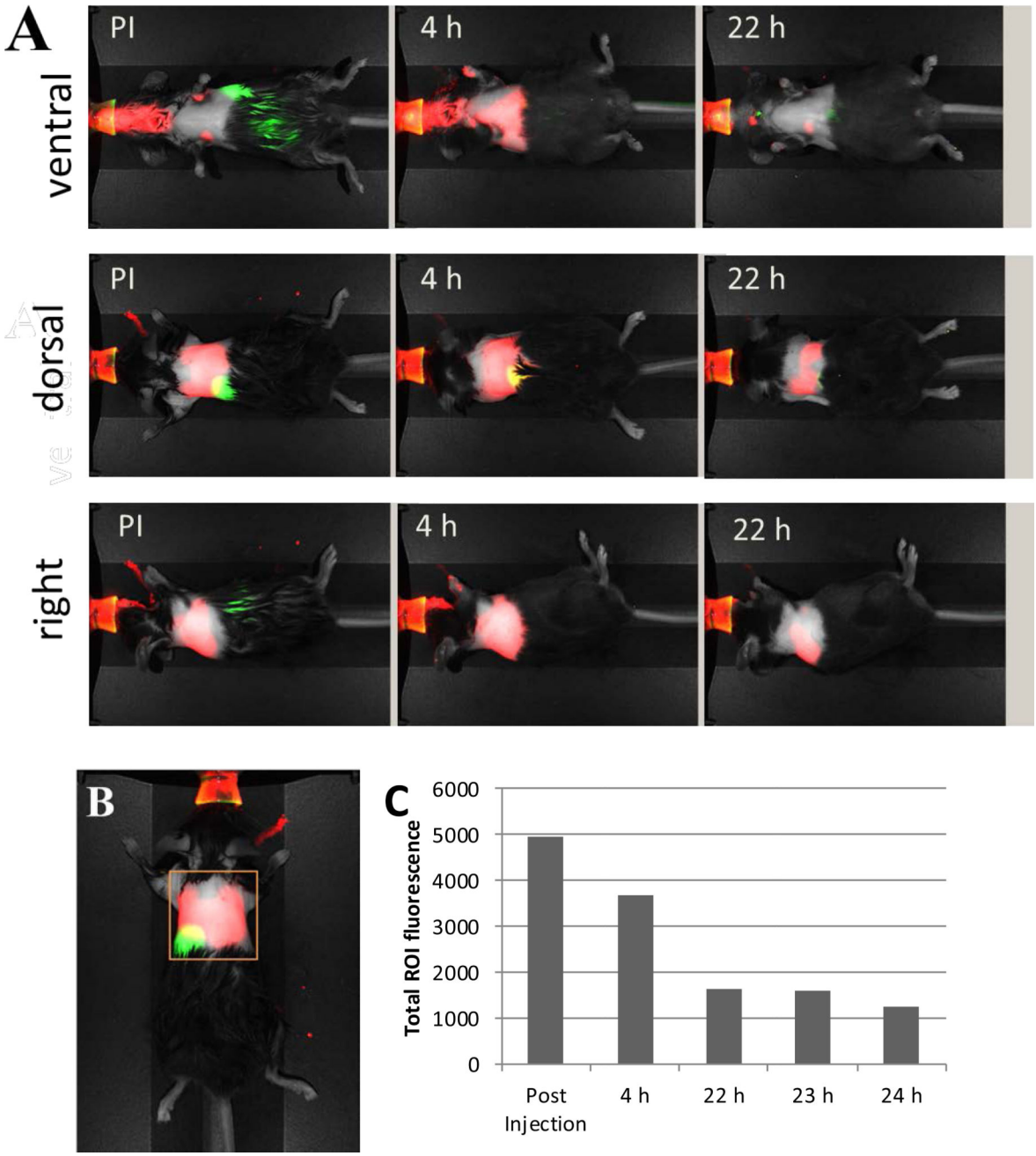

Figure 5.

A: Fluorescent dye cypate delivered IT shows retention in the lung area within 24 hours. Red - NIR fluorescence channel (785/810 nm), green –fluorescence channel (685/710 nm). B: Region of interest (ROI) C: change of total fluorescent signal with time (ROI, dorsal position). Fluorescence in the 700 nm region (green) originates from digestion of chlorophyll-containing food in the stomach and intestines. Fluorescence from chlorophyll-containing chow is much more intense at about 700 nm than 800 nm and identified the location of the stomach and intestine relative to the expected signal from the nanoparticles in the lungs.

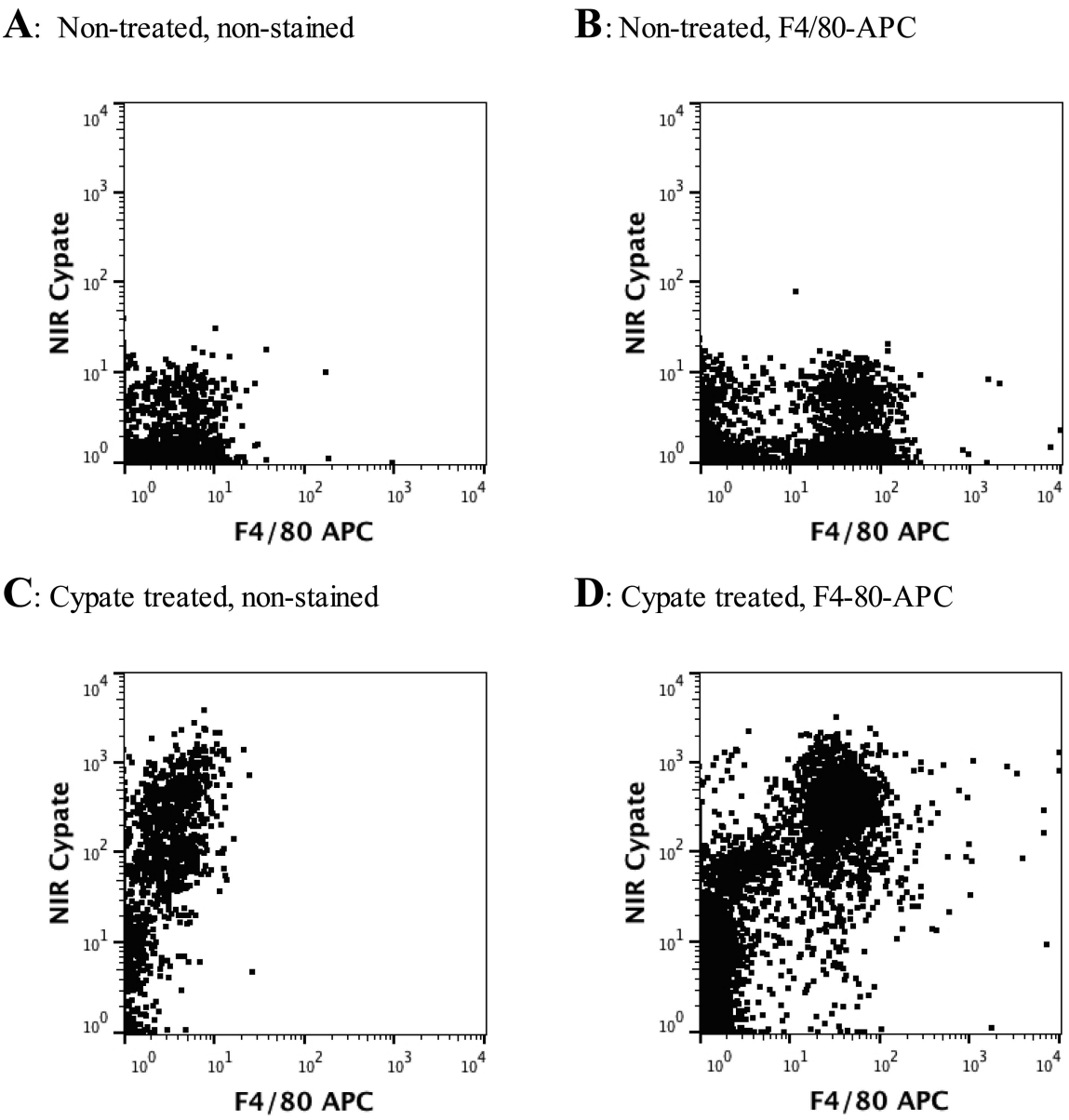

Figure 6.

Flow cytometry of bronchoalveolar lavage cells: not treated with cypate (A-B) and 4 hours after cypate treatment (C-D). Y-axis – NIR channel, X-axis – APC channel